Magnetic Field Crosstalk Suppression Method on Superconducting Quantum Chips

Yan Ye[1], Jiangtao Liu[2], Xiaoqiang Hou[2], Jianqiong Zhang[3] and ZhiZhuo Huang[3]

[1]Beijing Metro Operation Administration Corporation Limited. Beijing, China
[2]CRRC Qingdao Sifang Co.,Ltd. Qingdao, China
[3]Southwest Jiaotong University. Chengdu,China

13001957600@163.com

Abstract. The arithmetic power of a quantum computer is determined by a combination of the number of quantum bits and the fidelity of a single bit. Superconducting quantum chips can be prepared using a process similar to that of semiconductor chips, and are therefore of interest because of their natural advantages in terms of scalability. However, as the number of quantum bits increases, the z-control lines (magnetic field control lines) on the superconducting quantum chip also increase, leading to increased magnetic field crosstalk between individual control lines, which affects the fidelity of a single bit and further affects the arithmetic power of superconducting quantum computing. To address the above problems, this paper proposes two methods to reduce the magnetic field crosstalk between the control lines by modeling and simulating the superconducting quantum chip using air bridges and inflow structures, and the simulation results show that the magnetic field crosstalk between the control lines is significantly improved after the introduction of air bridges and inflow structures. This work provides a basis for further suppression of magnetic field crosstalk between the z-control lines of superconducting quantum chips.

1. Introduction

Quantum computers have attractive application prospects in public key password cracking and new drug development. As the most promising current implementation, superconducting quantum computers have advantages such as large-scale scalability because their implementation processes are compatible with existing semiconductor processes. In order to improve its performance, the fidelity of the quantum chip needs to be improved on the one hand, and the number of quantum bits on the chip needs to be increased on the other. The number of control lines on a quantum chip increases proportionally with the number of quantum bits, which increases the magnetic interference between control lines and thus leads to a decrease in the fidelity of the quantum chip, i.e., a decrease in the performance of the quantum computer. Therefore, it is important to study the crosstalk between control lines.

In 1980, Paul Benioff at Argonne National Laboratory was the first to throw out the new concept of quantum computing and developed a quantum Turing machine with a classical analog based on this idea, which is usually considered as the prototype of quantum computer[1]. 1982, Feynman continued to enrich Benioff's s theory and proposed the idea that quantum systems could be simulated by designing

a quantum computer based on quantum principles, which is unanimously considered by experts and scholars in the field of quantum computing as the earliest idea of quantum computers[2].

In 2017 IBM held a conference to announce the launch of the world's first commercial "universal" quantum computing service system, IBM O. IBM explained that the service is equipped with the ability to be accessed directly over the Internet and that the system has a transformative role in drug development and various scientific research. IBM explained that the service is equipped with direct Internet access and that the system has a transformative impact on drug development and scientific research, and has begun soliciting consumer users. In addition to IBM, other companies, such as Intel, MIT, ETH, Google and Microsoft, are also exploring the field of practical quantum computers [3,4,5].

Google released in 2019 a quantum chip called "Sycamore", which is the first experimental demonstration of the superiority of quantum computers over traditional classical architectures, and this chip containing 54 quantum bits was announced to achieve "quantum hegemony"[6]. Quantum hegemony refers to the computational power possessed by quantum computing that surpasses that of all conventional computers.

On December 4, 2020, Pan Jianwei's team at the University of Science and Technology of China (USTC) announced the design and implementation of a quantum computing prototype containing 76 quantum bits - "Nine Chapters" - and announced the realization of the "quantum hegemony" through a demonstration computational display of the algorithm of Gaussian Boson sampling. "This breakthrough makes China the second country in the world to achieve "quantum hegemony" [7,8].

Superconducting quantum computing has become an international hot topic, but this technology is still in a nascent stage, and there are still many technical problems to be broken through one by one. In a superconducting quantum chip, each superconducting quantum bit is located on a cross capacitor, and the state of the superconducting quantum bit is regulated by a set of chip control lines connected in parallel with it (see Figure 1 for the specific structure). This state modulation consists in two aspects:

1) The first aspect refers to the application of an excitation modulation signal (i.e., xy-control) to the chip control line for excitation to change the state of the superconducting quantum bit.

2) The second aspect refers to the application of a bias flux current signal to the chip control line via a flux modulation line (i.e., z-control) for tuning the frequency of the superconducting quantum bits.

Wherein: said bias flux current signal is usually provided directly with a constant current voltage source and the magnetic flux of the chip control line is varied by an applied constant bias flux current or by mutual inductive coupling with the chip control line, which in turn modulates the frequency of the superconducting quantum bits containing the control line of this superconducting quantum chip[9].

The research in this paper focuses on investigating the flux crosstalk phenomenon on the Z control line and testing the effectiveness of two structural solutions to suppress magnetic field crosstalk.

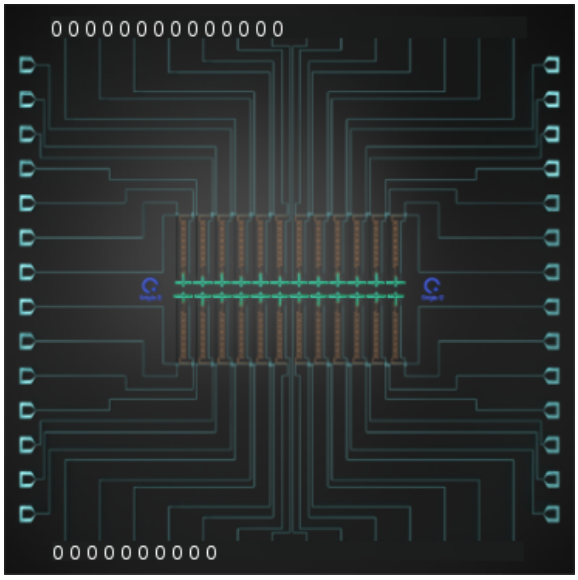

Figure 1. Kuafu KF C24-100 quantum chip

2. Chip control line modeling

2.1. Basic structure

For the time being, the complex structure of the chip and the influence of the working environment are not considered, and only a single control line model structure is established to explore the magnetic flux density distribution near it and verify the correctness of the simulation setup. In this scheme, a control line model of similar size to the actual chip is considered, and then three monitoring lines are inserted at 40um and 2mm from the control line terminal. These three pairs of detection lines are located 10um above the control line, through the middle of the control line, and 10um below the control line, and the low-frequency magnetic field crosstalk phenomenon on the three pairs of monitoring lines is detected by applying a voltage excitation of 1.0nV to the chip.

As shown in Figure 2, the dielectric plate model is established in the studio, and the dielectric plate is divided into two parts: dielectric substrate and superconducting layer, and the dielectric substrate is made of sapphire (excellent electrical insulation performance, hexagonal symmetric structure, stable chemical performance, and excellent superconducting substrate material) with a dielectric constant of 11.5; the superconducting layer material is made of aluminum, which shows superconducting characteristics at 1.196K, and the existing superconducting quantum chip at The operating temperature is about 10mK, which is the most commonly used superconducting material for the preparation of superconducting quantum chips. Theoretically, the superconducting conductivity is infinite and the magnetic permeability is 0. However, since the model simulation will report errors when run under this condition, the conductivity is set to 1×10^10 S/m and the magnetic permeability is 1×10^(-10)H/m to approximate the ideal condition.

The chip control line model is established on the surface of the dielectric plate, the dielectric plate size is 5mm×5mm×0.5mm. The chip control line structure is shown in Figure 2, the surface superconducting layer thickness t is 100nm, the control line single line length is 2060um, a voltage port excitation of 1nV is applied to the control line, and the working environment is set to vacuum environment. The model is shown in Figure 2.

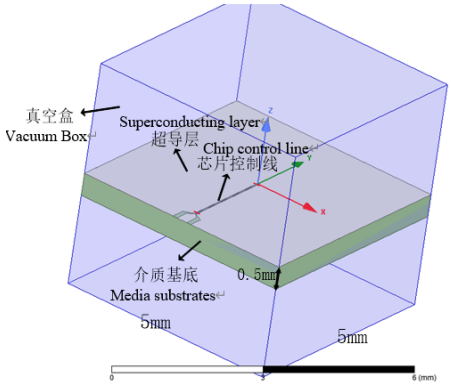

Figure 2. Simple model of single control line

2.2. Single control line result

The magnetic field distributions of the two monitoring lines A2 and B2 that pass through the middle of the control line (z-coordinate t/2) are shown in Fig. 4, with magnetic induction intensity maxima of -175.1316 dB and -175.2354 dB, respectively.The values of magnetic induction intensity measured at the position of the monitoring line passing through the superconducting layer are much lower than the values of magnetic induction intensity inside the control line, which is due to the fact that the superconductor when entering the superconducting state all magnetic fields inside the superconductor are repelled and the magnetic field inside the superconductor always remains zero, a phenomenon known as the Meissner effect[10]. However, since the superconducting layer is not set to the ideal condition in the simulation, the magnetic induction intensity value in the superconducting layer does not become 0. However, the magnetic field in the superconducting layer is much smaller than the magnetic field in the medium, indicating that our simulation setup is correct.

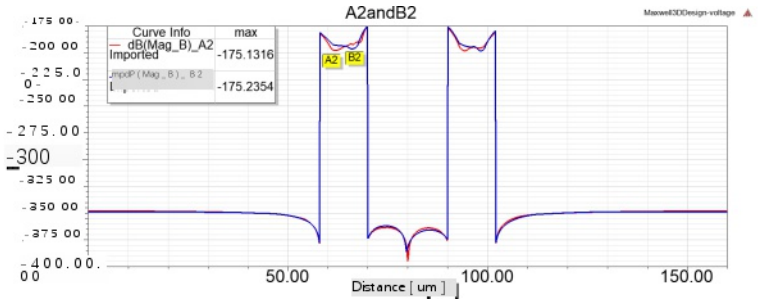

Figure 3. Distribution of magnetic induction intensity of Group 2 monitoring lines

3. The diversion structure suppresses magnetic field crosstalk

Due to the limitation of chip size, the chip control line spacing cannot be increased indefinitely. In order to reduce the crosstalk phenomenon of magnetic field, it is necessary to consider from the perspective of control line structure, so this paper gives a scheme of adding a guide structure between two groups of control lines to form a circulating field between the guide structure and the control line structure, so that the magnetic induction intensity distribution near the Josephson junction on the cross capacitor is more stable.

In order to closely match the structure size of the actual chip control lines, this scheme will set the control line spacing to 500um in the subsequent simulation operation, and set one monitoring line for each group of control line models, which is set on the surface of the cross capacitor, between the superconducting layer and the substrate material. The size and position of the conductive structure are shown in Figure 3, and the thickness of the conductive structure is the same as the thickness of the control line and the cross capacitor, which are both 100nm.

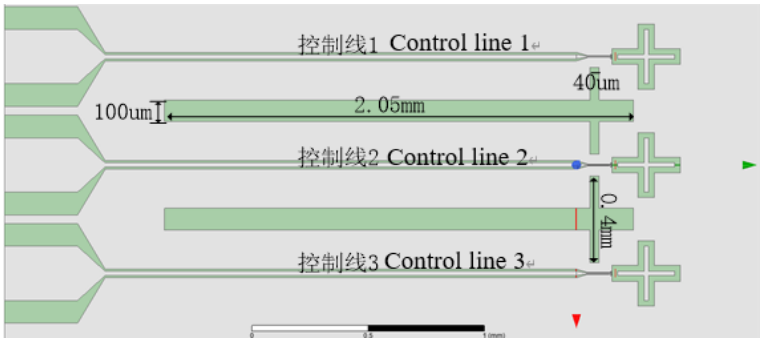

Figure 4. Schematic diagram of diversion structure dimensions

3.1. The first set of incentive results

In the case of the first set of excitation without the addition of the current guide structure, the difference in magnetic induction intensity between monitoring lines 1 and 2 is about 15 dB and between monitoring lines 1 and 3 is about 18 dB when the control line spacing is 500 um. After the addition of the current guide structure, the difference in magnetic induction intensity between monitoring lines 1 and 2 is about 25 dB and between monitoring lines 1 and 3 is about 28 dB (See Figure 5). In general, the magnetic induction intensity on monitoring lines 2 and 3 decreased by about 10 dB relative to the result before the addition of the current guide.

The distribution of magnetic inductance on the chip surface in Figure 6 shows that the magnetic inductance near the cross capacitor is more uniform and stable after the addition of the current guide structure, indicating that the current guide structure plays a good role in crosstalk suppression.

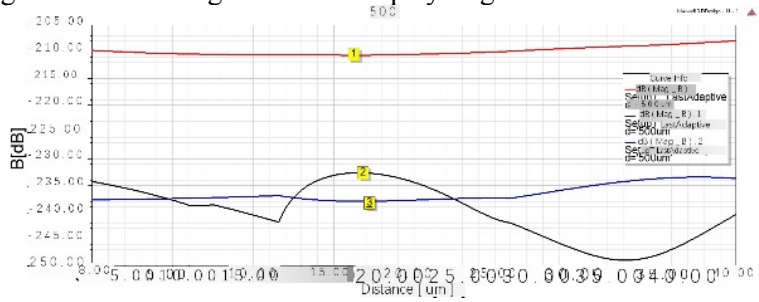

Figure 5. Variation curve of magnetic induction intensity

3.2. The second set of incentive results

In the case of the second set of excitation without the current-conducting structure, the difference in magnetic induction intensity between monitoring lines 1 and 2 is about 4.5 dB and between monitoring lines 2 and 3 is about 3 dB when the control line spacing is 500 um. After adding the current-conducting structure, the difference in magnetic induction intensity between monitoring lines 1 and 2 is about 7 dB and between monitoring lines 2 and 3 is about 12 dB (see Fig. 6). The magnetic induction intensity change between monitoring lines 2 and 3 is more obvious due to the fact that the inflow structure creates a circulating flow field between control line 2 and control line 3, which makes the distribution of the excitation flow weaker near the cross capacitor 3, thus reducing the magnetic induction intensity distribution near the cross capacitor 3.

The distribution of magnetic induction intensity on the chip surface in Fig. 7 also shows that the crosstalk of the magnetic field between cross capacitor 2 and cross capacitor 3 is improved by adding the inflow structure.

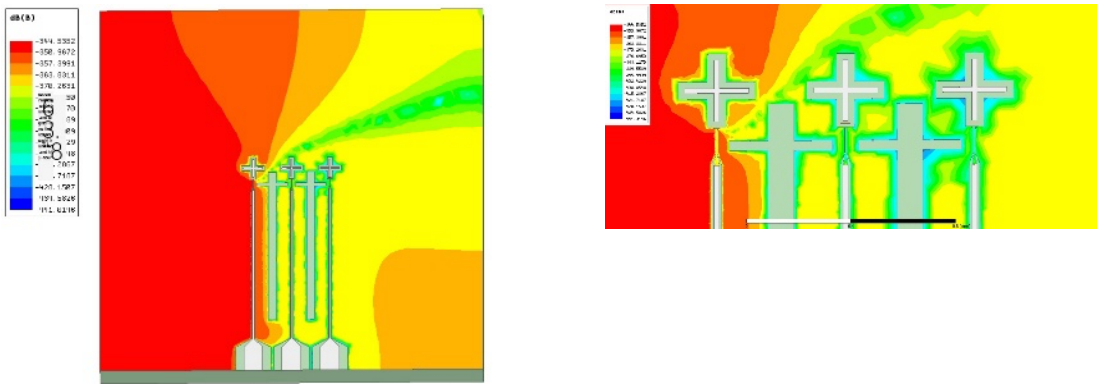

(a) Chip surface distribution map (b) Distribution diagram near cross capacitance

Figure 6. Distribution of magnetic induction intensity of the first group of excitation

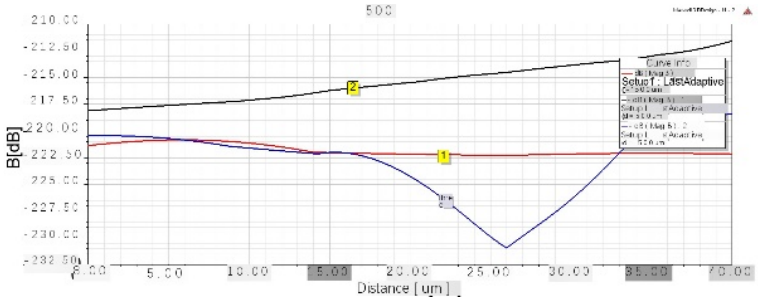

Figure 7. Variation curve of magnetic induction intensity

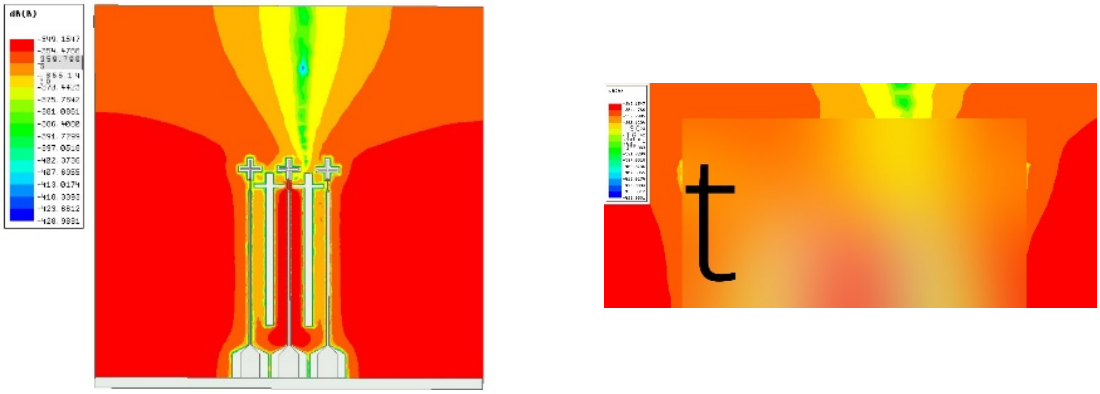

(a) Chip surface distribution map (b) Distribution diagram near cross capacitance

Figure 8. Distribution of magnetic induction intensity of the second group of excitation

3.3. The third group of incentive results

In the case of the third set of excitation without the addition of the current guide structure, the difference in magnetic induction intensity between monitoring lines 1 and 3 is about 12 dB and between monitoring lines 2 and 3 is about 8.5 dB when the control line spacing is 500 um. After the addition of the current guide structure, the difference in magnetic induction intensity between monitoring lines 1 and 3 is about 17 dB and between control lines 2 and 3 is about 20 dB (See Figure 9). The magnetic induction intensity of monitoring line 2 is slightly lower than that of monitoring line 1. In addition to the influence of the inflow structure, the reason also includes the error of gridding, because the number of gridding of the cross capacitor is not enough, which makes the variation curve of magnetic induction intensity on the monitoring line not smooth enough, and there is a certain error in the value, but this error has less influence on the conclusion, and in order to save simulation resources, the grid has not been optimized in this paper In order to save simulation resources, the grid has not been optimized in this paper.

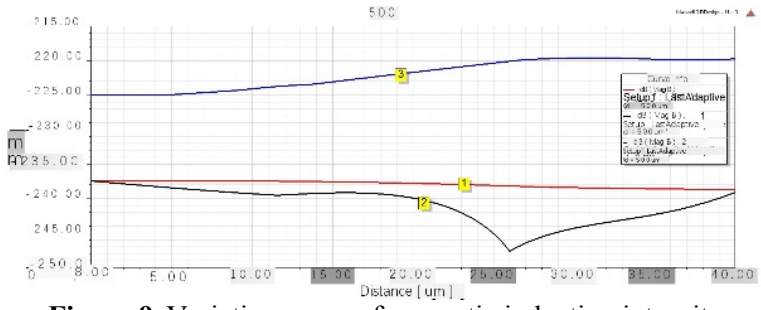

Figure 9. Variation curve of magnetic induction intensity

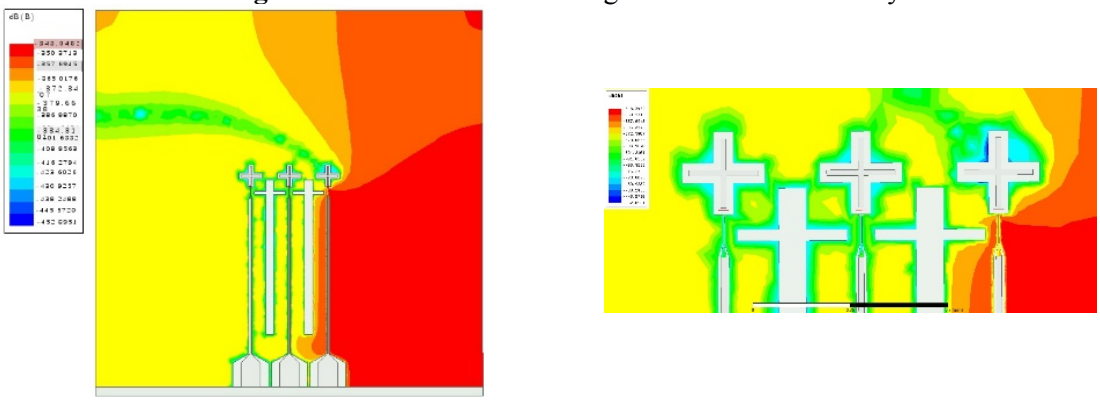

(a) Chip surface distribution map (b) Distribution diagram near cross capacitance

Figure 10. Distribution of magnetic induction intensity of the third group of excitation

4. Air Bridge Suppresses Magnetic field Crosstalk

Considering that the current distribution on both sides of the control line is uneven due to the current guiding effect of the capacitor junction on the excitation current, this paper gives a method to build air bridges on both sides of the capacitor junction of the control line. The air bridges are made of superconducting materials and connected to the superconducting layer, with the purpose of stabilizing the current distribution on both sides of the capacitor junction and forming a set of circulating currents through the air bridges, so as to stabilize the magnetic field distribution and reduce the magnetic field crosstalk. The air bridge is 30um wide, 30um high, and 10um line width, as shown in Figure 11(c). The simulation still uses a single-port excitation to compare the magnetic induction intensity distribution on the cross capacitor before and after adding the air bridge.

Compared with the actual superconducting quantum chip, the size of the air bridge in this simulation model is large, which is difficult to implement in reality, but it is simplified to save simulation resources.

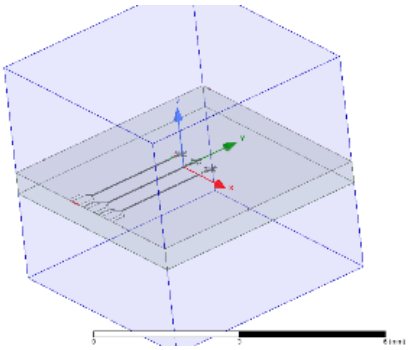

(a) Three sets of actual control line models

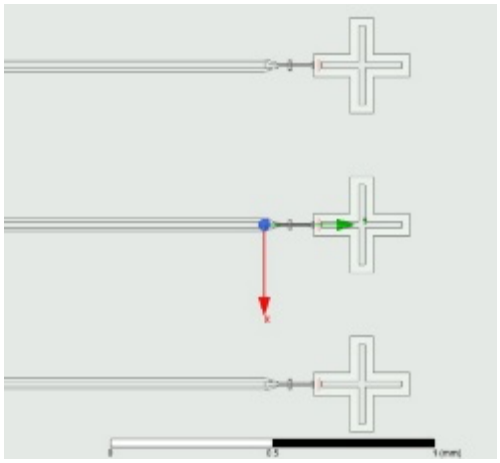

(b) Comparison of air bridge sizes

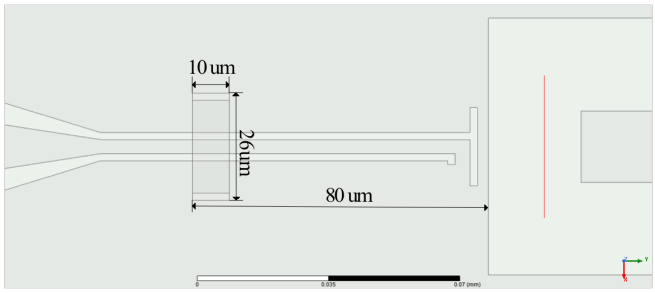

(c) Size of air bridge

Figure 11. Control line model of air bridge chip

4.1. The first set of incentive results

When the air bridge structure is not added, the magnetic induction intensity difference between monitoring lines 1 and 2 is about 15 dB and between monitoring lines 1 and 3 is about 18 dB for the first set of excitation when the control line spacing is 500 um. After the air bridge structure is added, the magnetic induction intensity difference between monitoring lines 1 and 2 is about 36 dB and between monitoring lines 1 and 3 is about 20 dB (see Figure 12). It can be seen that the air bridge has a good suppression effect on the crosstalk of the magnetic induction intensity on the monitoring lines.

Compared with the results of the magnetic induction intensity distribution in the first set of excitation cases with the deflector structure, the air bridge has a better effect on the magnetic field crosstalk suppression on monitoring lines 1 and 2, and the deflector structure has a better effect on the magnetic field crosstalk suppression on monitoring lines 1 and 3.

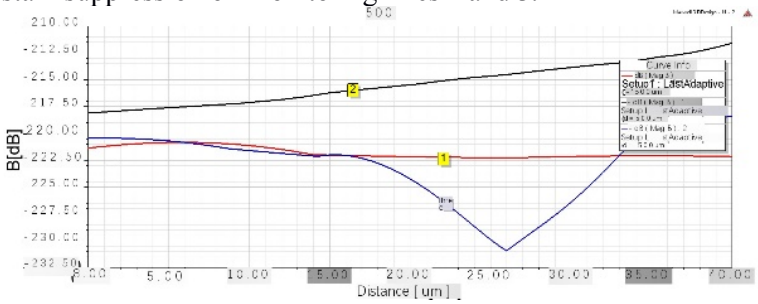

Figure 12. Variation curve of magnetic induction intensity

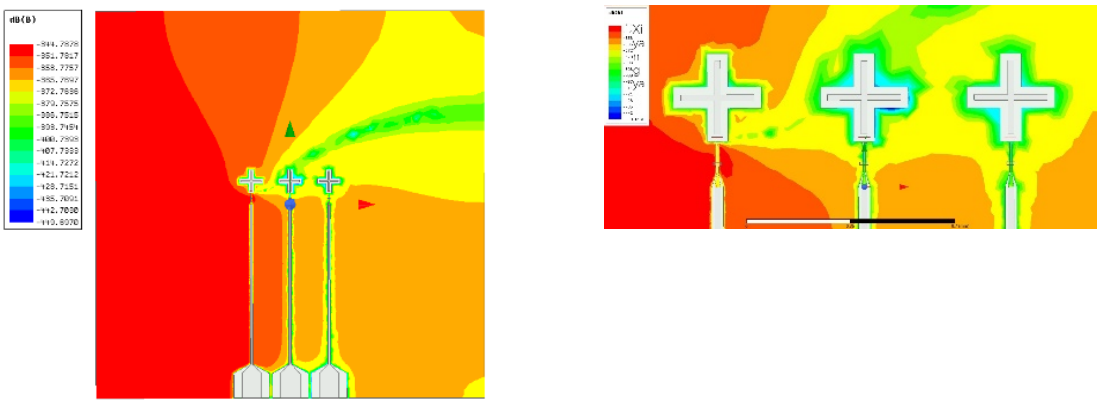

(a) Chip surface distribution map (b) Distribution diagram near cross capacitance

Figure 13. Distribution of magnetic induction intensity of the first group of excitation

4.2. The second group of incentive results

When the air bridge structure is not added, the magnetic induction intensity difference between monitoring lines 1 and 2 is about 4.5 dB and between monitoring lines 2 and 3 is about 3 dB in the second group excitation case when the control line spacing is 500 um. After adding the air bridge structure, the magnetic induction intensity difference between monitoring lines 1 and 2 is about 5 dB and between monitoring lines 2 and 3 is about 8.5 dB (See Figure 14). It can be seen that the air bridge also plays a good role in suppressing the crosstalk phenomenon of the magnetic induction intensity on the monitoring line.

Compared with the results of the magnetic induction intensity distribution in the second set of excitation cases with the inflow structure, the inflow structure has a better effect on the crosstalk suppression of the magnetic field on the three test lines.

Figure 14. Variation curve of magnetic induction intensity

4.3. The third group of incentive results

When the air bridge structure is not added, the magnetic induction intensity difference between monitoring lines 1 and 3 is about 12 dB and between monitoring lines 2 and 3 is about 8.5 dB for the third group excitation case when the control line spacing is 500 um. After adding the air bridge structure, the magnetic induction intensity difference between monitoring lines 1 and 3 is about 12 dB and between control lines 2 and 3 is about 10 dB (see Figure 16). It can be seen that the air bridge also plays a good role in suppressing the crosstalk phenomenon of magnetic induction intensity on the monitoring line.

In contrast to the magnetic induction intensity distribution results for the third set of excitation cases with the deflector structure, the deflector structure has a better suppression effect on the magnetic field crosstalk on the three test lines.

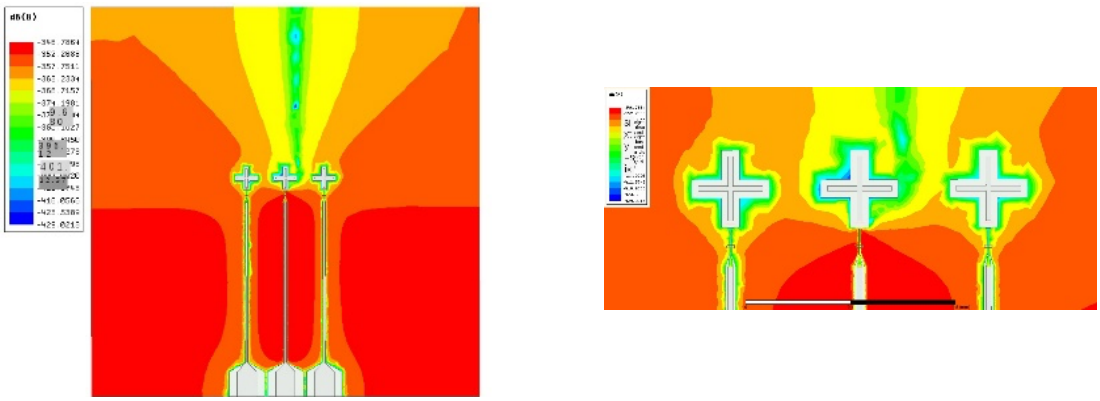

(a) Chip surface distribution map (b) Distribution diagram near cross capacitance

Figure 15. Distribution of magnetic induction intensity of the second group of excitation

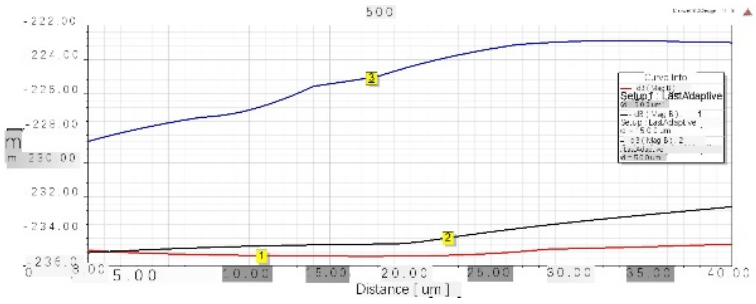

Figure 16. Variation curve of magnetic induction intensity

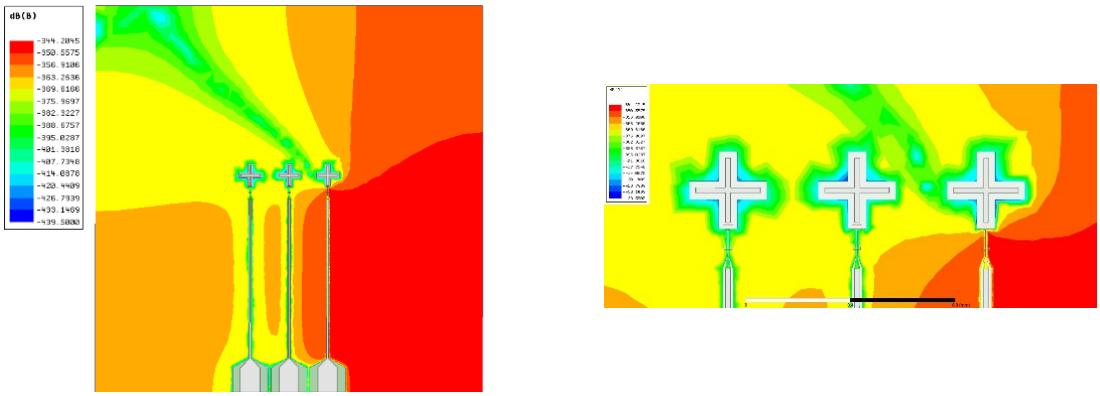

(a) Chip surface distribution map (b) Distribution diagram near cross capacitance

Figure 17. Distribution of magnetic induction intensity of the third group of excitation

5. Conclusion

To address the magnetic field crosstalk on superconducting quantum chips, this paper establishes the analysis method of magnetic field crosstalk on superconducting quantum chips by using electromagnetic simulation software, and further designs the inflow structure and air bridge structure to suppress the magnetic field crosstalk, and its simulation results show that both methods have certain suppression effect on the magnetic field crosstalk. This study is of great significance and reference value for solving the crosstalk on superconducting quantum chips and improving the single-bit fidelity of superconducting quantum chips, thus enhancing the arithmetic power of superconducting quantum computing.

6. References

[1] Wang Jilin, Liu Jianjian, Chen Peiyi. Quantum computing and superconducting quantum computers[J]. Micro and Nanoelectronics, 2009,46(06):321-326+345. Ying Jiang. Modeling and simulation of transponder systems and their applications[D]. Beijing Jiaotong University,2014.
[2] R. P. Feynman. Simulating physics with computers[J]. International Journal of Theoretical Physics,1982, 21: 6-7.
[3] Ren Jirong. Development and application prospects of quantum computers[J]. Electronic World, 2018,(1):97,99.
[4] Han, Zhexin, Gu, Guotai, Xiao, Han. Research and application of quantum computers[J]. Henan Science, 2015,(9):1559-1563.
[5] Zhang Jianfen. Conceptual principles and prospects of quantum computers[J]. Physics Bulletin, 2015,(4):125-128.
[6] Arute F, Arya K, Babbush R, et al. Quantum supremacy using a programmable superconducting processor[J]. Nature，2019，574: 505-510.
[7] Wang Jinlan. Chinese scientists achieve a milestone breakthrough in "quantum computing superiority"[J]. Science, 2021,73(01):43+2.
[8] Guo Guangcan, Chen Yipeng, Wang Qin. Advances in quantum computer research[J]. Journal of Nanjing University of Posts and Telecommunications (Natural Science Edition), 2020,40(05):3-10.
[9] Kong, Weicheng. A crosstalk analysis-based method for superconducting quantum bit modulation [P]. Anhui, China: CN110488091A,2019-11-22.
[10] Li Xiaohu. Preparation and performance study of superconducting JosephsonF Suidon junction and structural exploration of superconducting quantum bit circuits[D]. Nanjing University,2015.